

Velocity-selective coherent population trapping of two-level atoms

J. Hack,¹ L. Liu,¹ M. Olshanii,^{1,2} and H. Metcalf¹

¹*Physics and Astronomy, State University of New York, Stony Brook, New York 11794-3800*

²*Physics and Astronomy, University of Southern California, Los Angeles, California 90089-0484*

(Received 8 November 1999; published 12 June 2000)

We have demonstrated velocity-selective coherent population trapping (VSCPT) in a two-level system created by circularly polarized light driving the $2^3S_1 \rightarrow 3^3P_2$ transition in metastable helium. It is quite different from the usual VSCPT because there need be no consideration of selection rules, polarization, or internal atomic states. This most primitive case elicits the simple nature of VSCPT as a special kind of quantum interference, and demonstrates the presence of VSCPT in a system that has only two internal levels. It is readily observed for this transition because the ratio of the recoil frequency to the natural linewidth is 0.22, two orders of magnitude larger than for most laser cooling experiments. Our trapped state is fed by Doppler cooling, which is unusually effective here because of the large recoil, and is totally absent in previously described VSCPT experiments.

PACS number(s): 32.80.Pj

Laser cooling has routinely enabled the production of atomic vapors at only a few times the recoil temperature $T_r \equiv (\hbar k)^2 / M k_B \equiv 2\hbar \omega_r / k_B$ [1] (k_B is Boltzmann's constant, $k \equiv 2\pi/\lambda$, and λ is the wavelength of the atomic transition). Aside from evaporative cooling, which is not truly an optical technique, only two methods for producing temperatures below T_r have been demonstrated. These are velocity-selective coherent population trapping (VSCPT) [2] and Raman cooling [3]. The two main features of this paper are the demonstration of VSCPT with a two-level atom as anticipated in Ref. [4], and VSCPT fed by laser cooling, the goal of Refs. [5–7]. This technique avoids concerns about light polarization, the internal atomic quantum numbers, the Clebsch-Gordan coefficients, and the selection rules [4,8]. Therefore it elucidates the simplicity and beauty of the isolated phenomenon [9].

Adequate discussion of VSCPT requires a quantum mechanical description of the atomic motion. The classical description of laser cooling requires that the atomic phase space distribution can be split onto an ensemble of “classical wave packets” with area larger than \hbar in such a way that the atomic Hamiltonian does not vary significantly over the wave packet [10]. This is definitely not the case for subrecoil cooling. Below T_r the width of the momentum distribution is less than $\hbar k$ so the corresponding classical wave packet must extend over a range larger than λ .

This description begins by writing the total Hamiltonian as

$$\hat{\mathcal{H}} = \hat{\mathcal{H}}_{\text{atom}} + \hat{\mathcal{V}}_{\text{atom-light}}, \quad (1)$$

where $\hat{\mathcal{H}}_{\text{atom}} = \hat{\mathbf{P}}^2 / 2M - \hbar \delta \hat{\mathcal{Q}}_e$ includes both the center-of-mass kinetic energy of the atom and the internal energy, $\delta \equiv \omega_{\text{laser}} - \omega_{\text{atom}}$ is the detuning of the laser from the atomic transition, $\hat{\mathcal{Q}}_e = \sum_e |e\rangle\langle e|$ is an operator describing a projection onto the excited state subspace and implies the rotating wave approximation, and $\hat{\mathcal{V}}_{\text{atom-light}} = -\hat{\mathbf{d}} \cdot \mathbf{E}(\hat{\mathbf{r}})$ describes the interaction of the atomic dipole $\hat{\mathbf{d}}$ with an external laser field of amplitude $\mathbf{E}(\mathbf{r})$. The basis states must then be labeled by

both internal (g, e) and external (p) quantum numbers, and are denoted by $|g; p\rangle$ or $|e; p'\rangle$.

The lifetimes of the basis states are no longer infinite because of optical excitation followed by spontaneous emission that causes the atoms to diffuse among the momentum states. The escape rate of the state $|\psi\rangle$ from one momentum to another is denoted by Γ_ψ , and is rigorously defined as the probability $\Gamma_\psi dt$ that an escape from $|\psi\rangle$ happens within a time interval dt . This escape rate is proportional to the fraction of the excited state component in the state of interest: $\Gamma_\psi = \langle \psi | \hat{\mathcal{Q}}_e | \psi \rangle \gamma$.

Previous discussions of the mechanism of velocity-selective trapping in VSCPT have always been predicated on the existence of a noncoupled, stationary state $|\text{NC}\rangle$ (dark state). The lifetime of $|\text{NC}\rangle$ is limited only by external considerations [11]. Once atoms enter $|\text{NC}\rangle$ they cannot be excited out of it so the dynamics of such dark states has been described in terms of Levy flights [12].

One of the main results of this paper is the demonstration of VSCPT in a two-level atom where there is laser cooling toward the states of interest. In the usual $J=1 \rightarrow 1$ transition there is no cooling as discussed below, but the two-level atom scheme we use indeed benefits from very effective Doppler cooling [4]. VSCPT arises in our scheme because there are weakly coupled states $|\text{WC}(\mathcal{P})\rangle$ of a two-level atom that satisfy less stringent requirements than $|\text{NC}\rangle$. These states have a longer lifetime $\tau_{\text{WC}} \equiv 1/\Gamma_{\text{WC}}$ than neighboring momentum states, which is caused by a destructive interference in the excitation channel arising from the coherent superposition of different states $|g; p_i\rangle$.

Interference is characteristic of all quantum systems, and in our case it comes from the mixing of two degenerate momentum states by the standing wave light field. This mixing is caused by absorption of light by $|g; p\rangle$ followed by stimulated emission into $|g; p''\rangle$. Conservation of momentum requires $p - p'' = \pm 2\hbar k$. Since the absorption-stimulated emission process leaves the field energy unchanged and the atoms in their ground states, energy degeneracy requires that $4\hbar k(p \pm \hbar k)/2M = 0$. These two conditions can be met only by $p = \mp \hbar k$.

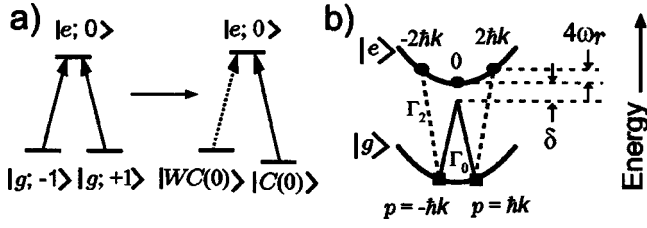


FIG. 1. (a) Schematic diagram of the transformation of the eigenfunctions from the bare atomic states to the eigenstates $|WC(\mathcal{P})\rangle$ and $|C(\mathcal{P})\rangle$. The optical coupling mixes the degenerate bare states $|g;p\rangle$ and $|g;p''\rangle$, so the eigenstates of \mathcal{H} are the non-degenerate $|WC(\mathcal{P})\rangle$ and $|C(\mathcal{P})\rangle$. The state $|C(\mathcal{P})\rangle$ is light shifted down because $\delta < 0$. (b) The parabolas show the kinetic energies of the states $|g;p\rangle$ and $|e;p\rangle$ vs p , and the levels marked with squares on the lower one show the constituents of $|WC(0)\rangle$ and $|C(0)\rangle$. The dashed lines show the weaker transitions to $|e;\pm 2\rangle$, which are detuned from resonance by $4\omega_r$, more than those to $|e;0\rangle$ for $\delta < 0$.

In the lowest order of perturbation theory, the ground eigenstates of $\hat{\mathcal{H}}$ are the orthogonal superpositions of $|g;P-\hbar k\rangle$ and $|g;P+\hbar k\rangle$ given by

$$|WC(\mathcal{P})\rangle = \{|g;P-\hbar k\rangle - |g;P+\hbar k\rangle\} / \sqrt{2}$$

and

$$|C(\mathcal{P})\rangle = \{|g;P-\hbar k\rangle + |g;P+\hbar k\rangle\} / \sqrt{2}. \quad (2)$$

[see Fig. 1(a)]. Here \mathcal{P} is the average momentum of the constituents of $|WC(\mathcal{P})\rangle$ or $|C(\mathcal{P})\rangle$. It is straightforward to show that the excitation probability of $|WC(\mathcal{P})\rangle \rightarrow |e;P\rangle$, proportional to $|\langle e;P|\hat{\mathbf{d}} \cdot \mathbf{E}(\hat{\mathbf{r}})|WC(\mathcal{P})\rangle|^2$, vanishes because of the destructive interference of transition amplitudes. Then $|WC(\mathcal{P})\rangle$ is the longer-lived state in the neighborhood of $\mathcal{P} = 0$ [13].

Another escape route from $|WC(\mathcal{P})\rangle$ is the optical excitation $|WC(\mathcal{P})\rangle \rightarrow |e;\pm 2\hbar k\rangle$. (This is absent from the usual ‘‘closed family’’ description of ordinary VSCPT [14].) Because each component of $|WC(\mathcal{P})\rangle$ can only go to one of the states $|e;\pm 2\hbar k\rangle$, there is no interference of transition amplitudes. However, this transition is inhibited by its larger detuning for $\delta < 0$ [see Fig. 1(b)].

The excitation rates of the eigenstates in Eq. (2) are

$$\Gamma_C(0) \approx 2\Gamma_0 + \Gamma_2 \quad \text{and} \quad \Gamma_{WC}(0) \approx \Gamma_2, \quad (3)$$

as indicated in Fig. 1(b). These rates are calculated in the usual way, using the on-resonance saturation parameter $s_0 \equiv I/I_s$, where $I_s \equiv \pi\hbar c/3\lambda^3\tau$ and I is the incident light intensity. The pumping rate of one beam is $\Gamma_p(\delta) \equiv (s_0\gamma/2)/[1+s_0+(2\delta/\gamma)^2]$ and so $\Gamma_0 = \Gamma_p(\delta + \omega_r)$ and $\Gamma_2 = \Gamma_p(\delta - 3\omega_r)$.

The contribution of ω_r to these excitation rates is of little consequence for the usual atomic transitions where $\epsilon \equiv \omega_r/\gamma \ll 1$, but is important for our case of $\epsilon \approx 0.22$ on the $2^3S \rightarrow 3^3P$ transition at $\lambda = 389$ nm of He*, where $4\omega_r \approx \gamma$ ($\tau \approx 107$ ns, $\omega_r \approx 330$ kHz). For this transition there is a

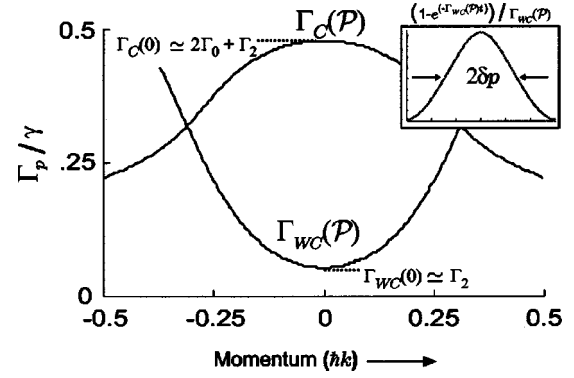


FIG. 2. A plot of the escape rates Γ_{WC} and Γ_C found by diagonalization of the Wigner-Weisskopf Hamiltonian for $s_0 = 0.4$, $\delta = \gamma/2$. There are five states in the calculation but only $|WC\rangle$ and $|C\rangle$ are shown. The inset shows the momentum distribution of a single peak for this case.

wide range of values of δ and s_0 where $\Gamma_{WC}(0)$ is smaller than $\Gamma_C(0)$ by a factor of 8 or more.

The discussion above follows previous treatments of VSCPT [2,14,15] where the noncoupled state $|NC\rangle$ appears in place of $|WC\rangle$. However, there are two significant differences between these cases and our experiment. First, instead of depending on a random walk in momentum space to populate the VSCPT state, there is Doppler cooling, which is absent in the $J=1 \rightarrow 1$ case. Second, since $|WC\rangle$ is not truly a dark state because $\Gamma_2 \neq 0$, the Levy flight description of VSCPT does not apply [12] because of the optical pumping: $\Gamma_{WC}(0) \neq 0$.

For $\mathcal{P} \neq 0$, the two ground state components of $|WC(\mathcal{P})\rangle$ are no longer degenerate and their relative phase oscillates [2]. The destructive interference that causes the longer lifetime of $|WC(\mathcal{P})\rangle$ disappears and so the state can evolve into $|C(\mathcal{P})\rangle$. This contribution to the loss rate from $|WC(\mathcal{P})\rangle$ depends on $|\langle WC(\mathcal{P})|\hat{\mathbf{P}}^2/2M|C(\mathcal{P})\rangle|^2$ and is given by [15] $\Gamma_{WC}(\mathcal{P}) \approx \Gamma_{WC}(0) + \Gamma_0''(\mathcal{P})$, where $\Gamma_0''(\mathcal{P}) \equiv 16\epsilon^2\gamma\mathcal{P}^2/[(\hbar k)^2 s(0)]$ for the $J=1 \rightarrow 1$ case. Thus the long lifetime of $|WC(\mathcal{P})\rangle$ is clearly velocity selective because it decreases with increasing \mathcal{P} .

To address our two-level atom case, we have expanded the perturbative treatment of Ref. [15] by numerical diagonalization of the effective Wigner-Weisskopf Hamiltonian $\hat{\mathcal{H}}_{WW} = \hat{\mathcal{H}} - i\hat{Q}_e\gamma/2$. This was done in a subspace of the five states $|g;P\pm\hbar k\rangle$, $|e;P\rangle$, and $|e;P\pm 2\hbar k\rangle$ that are significantly involved in our experiment. We found eigenstates similar to those of Eq. (2), and identified the imaginary part of their eigenenergies $-2\text{Im}\{E_{WC}(\mathcal{P})\}/\hbar$ with their total escape rates $\Gamma_i(\mathcal{P})$ (plotted in Fig. 2). For the state corresponding to $|WC(\mathcal{P})\rangle$, $\Gamma_{WC}(\mathcal{P})$ is indeed a minimum at $\mathcal{P} = 0$.

We can use the \mathcal{P} dependence of $\Gamma_{WC}(\mathcal{P})$ to estimate the width of the two cooled peaks in our VSCPT signal. Following the ‘‘reservoir model’’ of Ref. [11], we assume that $|WC(\mathcal{P})\rangle$ is fed by a uniform flow $\dot{\rho}$. Then the time evolution of the momentum distribution $N(\mathcal{P})$ is

$$N(\mathcal{P}, t) = \{\dot{\rho}(1 - e^{-\Gamma_{WC}(\mathcal{P})t})/\Gamma_{WC}(\mathcal{P})\} \quad (4)$$

where t is the interaction time (see inset to Fig. 2). The full width at half maximum can be calculated directly from $N(\mathcal{P})/\dot{\rho}$.

In our apparatus a beam of about 10^{14} He*/s sr is generated in a dc discharge followed by a set of apertures. The atoms have average velocity of about 1100 m/s and spread of about ± 200 m/s [16]. Atoms then enter an interaction region where the magnetic field is controlled to \pm a few μ T. Here they cross a variable width standing wave of circularly polarized $\lambda = 389$ nm light produced by frequency doubling light from a Ti:sapphire laser using an external buildup cavity. The light drives the $J=1 \rightarrow 2$ component of the $2^3S \rightarrow 3^3P$ transition of He*.

We produce an effective two-level atom using circularly polarized light along the \hat{z} direction. Then optical pumping populates the $2^3S_1(M_J=+1)$ state which can only be excited to the $3^3P_2(M_J=+2)$ state via the cycling transition, thus producing a closed, two-level system that is subject to laser cooling.

Next the atoms fly freely for 1.4 m where they impinge on a multichannel plate and their 20 eV of internal energy causes the release of electrons. The subsequently amplified electron shower is accelerated to a phosphor screen and a visible image is formed. This image is captured by a charge-coupled device camera outside the vacuum system and is recorded using a PC with a frame grabber card. We sum each column of pixels in the direction perpendicular to the transverse motion of the atoms in order to average over the vertical direction of the image to determine the one-dimensional spatial profile of the beam, and the transverse velocity of the atoms resulting from their interaction with the transverse laser beam is inferred.

A typical result is shown in Fig. 3. The dominant features are the tall Doppler-cooled peak near $v=0$ and the dips on either side from where these atoms were captured. The capture range for the Doppler cooling is $\gamma/k = v_D/\sqrt{\epsilon} \sim v_D/2$ where $v_D = \sqrt{\hbar\gamma/2M}$ is the Doppler cooling limit. When these two features are fitted with Gaussians of different signs and widths and then subtracted, there remains a small two-peaked signal and an uncomfortably wiggly baseline. But if the two-peaked VSCPT signal is included directly in the fitted line shape, the sum of the squares of the residuals drops by typically a factor of 10, and the baseline is nearly flat. The scale for all plots in Fig. 3 is the same, showing that about half the atoms are collected into $|WC(0)\rangle$ as a result of the laser cooling.

In the usual case of VSCPT [2,14] in the $2^3S_1 \rightarrow 3^3P_1$ transition in He* at $\lambda = 1.083 \mu\text{m}$, there is no damping force because the Doppler and polarization gradient cooling cancel one another as a result of a numerical ‘‘accident’’ [17] (up to now all VSCPT experiments have been done on a $J=1 \rightarrow 1$ transition). Atoms can populate this usual VSCPT state only by a random walk in momentum space resulting from scattering light, and if their average momentum diffuses very far from $\pm \hbar k$, they have only a small chance to return during the interaction time. We have observed similar VSCPT for the $2^3S_1 \rightarrow 3^3P_1$ transition at $\lambda = 389$ nm, and a sample of our data is shown as an inset to Fig. 3. (There are special

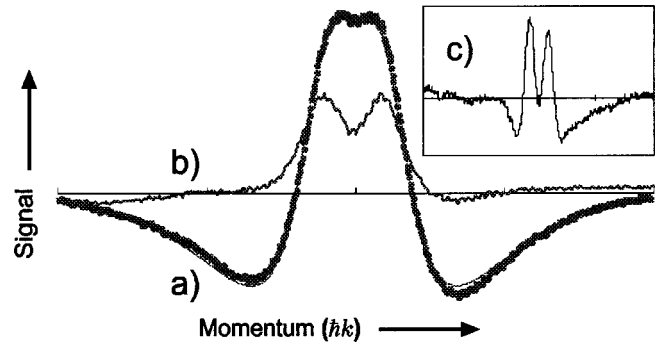


FIG. 3. A single frame taken in 1/30 s of the two-level atom VSCPT in a circularly polarized standing wave at $\lambda = 389$ nm. The deep dips on either side of the Doppler-cooled central peak show the capture range of the strong cooling at this detuning of -1.5γ and saturation parameter $s_0 = 0.75$. The background signal of the atomic beam shape in the absence of laser light has been subtracted, but there has been no smoothing. (a) The data points overlay the fitted curve with two Gaussians for the cooling and two for the VSCPT extremely well (see text), but any of several other line-shape combinations gave significantly worse fits. (b) The two-peaked plot results from subtracting the Gaussians obtained using the full fit from the raw data. It indicates that about half the atoms are in $|WC\rangle$. The peaks are approximately $700 \mu\text{m}$ apart on the phosphor screen. The inset (c) shows ordinary VSCPT on the $J=1 \rightarrow 1$ transition at $\lambda = 389$ nm, with $\delta = 0.25\gamma$ and $s_0 = 0.4$. Their sharpness supports our claim that our instrumental resolution is of little consequence.

polarization configurations that do indeed combine VSCPT with a damping force [5,6], and this has been observed [7].)

By contrast, in our two-level atom experiment there is strong Doppler cooling because of the $J=1 \rightarrow 2$ transition. This cooling is very effective, nearly reaching T_r (which is $\ll T_D$ in most atoms) because the large value of ϵ makes the Doppler limit $T_D = \hbar\gamma/2k_B \approx 36 \mu\text{K}$, not very different from $T_r \approx 32 \mu\text{K}$. This is manifest as large atomic populations near $v=0$ in all of our data taken with $\delta < 0$, of which Fig. 3 is one example.

We can compare the observed widths of the VSCPT peaks with the predictions of the ‘‘reservoir model’’ of Eq. (4). The calculated widths are slightly corrected by adding in quadrature the instrumental width $\delta p_{inst} \approx \hbar k/3$. This comes from the longitudinal spread of velocities in our beam given by $\delta v/v \approx 2/11$ (half width at half maximum) and the resolution of the imaging detector. Its magnitude is confirmed by the very narrow VSCPT peaks shown as an inset to Fig. 3. There is excellent agreement between the measured and calculated VSCPT widths over a wide range of laser parameters. Since these widths are considerably larger than δp_{inst} , we conclude that the measured width is dominated by the VSCPT process and not by experimental limitations for most of our data.

We have performed numerous tests to support the claim that this is truly VSCPT. For example, Fig. 4 shows a series of signals similar to that of Fig. 3 taken at different values of detuning δ . The model above would predict that the escape rate from $|WC(\mathcal{P})\rangle$ is very much larger for $\delta > 0$ than for $\delta < 0$ because excitation to $|e; \pm 2\rangle$ is no longer off reso-

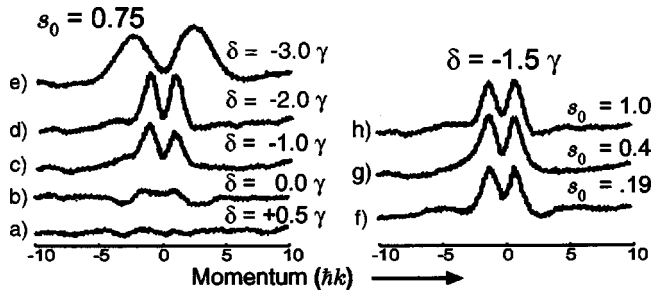


FIG. 4. A sequence of signals similar to that of Fig. 3 taken at different values of the detuning. For these 1/30 s pictures on the left, $s_0 = 0.75$, and for those on the right, $\delta = -1.5\gamma$. The background has been subtracted, but there has been no smoothing. For the largest detuning on the left ($\delta = -3\gamma$) the VSCPT signal is overwhelmed by the widely separated peaks of transient Doppler cooling at large δ . It is easy to see that the time required for a velocity change of γ/k is $\sim 1/2\epsilon\Gamma_p$. For a detuning of $\delta = -3\gamma$ this is nearly twice as long as our interaction time of about 100τ since $\Gamma_p \sim \gamma/100$. Thus atoms are not decelerated to the vicinity of $v = \pm \hbar k/M$, but instead pile up near the edge of the Doppler cooling range of $v = \pm(\delta - \gamma)/k = \pm 2\gamma/k$. By contrast, for $\delta = -2\gamma$ the atoms need a smaller velocity change to reach the recoil region and $\Gamma_p \sim \gamma/40$, so most atoms can be decelerated to the neighborhood of $p = \hbar k/M$. In this case they are readily optically pumped into $|WC\rangle$. Our data run in $(1/2)\gamma$ steps but are not all shown here.

nance by as much [see Fig. 1(b)]. This is clearly shown in Fig. 4, where the VSCPT signal lingers as the detuning moves from 0 toward the red, but vanishes within $\gamma/2$ on the blue side (where the Doppler force produces weak heating).

In a second test, we reduced the interaction time from its full value of many times τ_{WC} (interaction length ~ 20 mm) in small steps to a fraction of τ_{WC} (2 mm). We found that the strength of the VSCPT signal depended on both this interaction length and the laser parameters in a way fully consistent with the values calculated from Eq. (4). We chose a few τ_{WC}

(5 mm) for most of our data, corresponding to only $5 \mu s$ or 50τ , so we could have a reasonably flat laser beam intensity profile.

In still another test, we applied a dc magnetic field in various directions. With ordinary VSCPT in a $\sigma^+ - \sigma^-$ light field ($J = 1 \rightarrow 1$), \vec{B} along \hat{z} simply shifts the two peaks together along \hat{v}_z , consistent with balancing their kinetic and Zeeman energies. The condition for this is $(E_{kin})_1 - (E_{kin})_2 = \Delta E_{Zeeman}$ (evaluated for $\Delta M_J = 2$), which corresponds to the average velocity $\mathcal{P}/M = \mu_B g_J B_z / \hbar k$. We have confirmed this experimentally. However, with a two-level atom, the field leaves the peaks unchanged because they belong to the same internal state (there is no M_J): only the effective δ is changed by the Zeeman shifts. For \vec{B} perpendicular to \hat{z} , the VSCPT signal is destroyed in the usual $J = 1 \rightarrow 1$ case because the ΔM_J selection rules are compromised, but is minimally affected in our two-level case because the ΔM_J selection rules do not apply.

Finally, we have performed quantum density matrix calculations for the velocity distribution of the atoms for various laser parameters [4]. We find quite good agreement with our measurements, for both the quasi-steady-state distribution and its time development.

We have described and demonstrated the essential features of the fascinating phenomenon of VSCPT in the simplest possible case [4]. It appears in a two-level atom that has no truly dark states, and enables laser cooling in a domain where the quantum description of atomic motion is required ($T < T_r$). In our case, its observation is facilitated by working in a region where the usual requirement for laser cooling, $\epsilon \ll 1$, is not satisfied.

ACKNOWLEDGMENTS

Financial support was provided by ONR and ARO.

- [1] H. Metcalf and P. van der Straten, *Laser Cooling and Trapping* (Springer-Verlag, New York, 1999).
- [2] A. Aspect *et al.*, Phys. Rev. Lett. **61**, 826 (1988).
- [3] M. Kasevich and S. Chu, Phys. Rev. Lett. **69**, 1741 (1992).
- [4] M. Doery *et al.*, Phys. Rev. A **51**, 4881 (1995).
- [5] M. Shahriar *et al.*, Opt. Commun. **103**, 453 (1993).
- [6] M. Shahriar *et al.*, Phys. Rev. A **48**, R4035 (1993).
- [7] M. Widmer *et al.*, Opt. Lett. **21**, 606 (1996).
- [8] H. Metcalf, Phys. Scr. **T70**, 57 (1997).
- [9] There are many ways to exploit atomic selection rules to produce an effective two-level atom in the laboratory.
- [10] J. Dalibard and C. Cohen-Tannoudji, J. Opt. Soc. Am. B **2**, 1707 (1985); see also, V.S. Letokhov, M.A. Ol'shanii, and Yu.B. Ovchinnikov, Quantum Opt. **7**, 5 (1995).
- [11] R. Dum and M. Olshani, Phys. Rev. A **55**, 1217 (1997).
- [12] F. Bardou *et al.*, Phys. Rev. Lett. **72**, 203 (1994).
- [13] An alternative and useful view of this dark state can be obtained by considering that its components $|g; \pm 1\rangle$ have well

defined momenta, and are therefore completely delocalized. Thus they can be viewed as counterpropagating de Broglie waves of the same frequency, therefore forming a standing de Broglie wave. Its fixed spatial phase relative to the optical standing wave formed by the light beams results in the vanishing of the spatial integral of the transition matrix element so that the state cannot be excited. For p not exactly equal to ± 1 , the de Broglie wave would then be drifting slowly relative to the laboratory-fixed optical standing wave.

- [14] A. Aspect *et al.*, J. Opt. Soc. Am. B **6**, 2112 (1989).
- [15] G. Morigi *et al.*, Phys. Rev. A **53**, 2616 (1996); E. Arimondo, in *Laser Manipulation of Atoms and Ions*, International School of Physics "Enrico Fermi," Course CXVIII, edited by E. Arimondo, W. Phillips, and F. Strumia (North-Holland, Amsterdam, 1992), p. 191.
- [16] M. Doery *et al.*, Phys. Rev. Lett. **72**, 2546 (1994).
- [17] C. Cohen-Tannoudji, in *Laser Manipulation of Atoms and Ions*, (Ref. [15]), p. 99.